Test of the Brink-Axel Hypothesis for the Pygmy Dipole Resonance

D. Martin,[1] P. von Neumann-Cosel,[1,*] A. Tamii,[2] N. Aoi,[2] S. Bassauer,[1] C. A. Bertulani,[3] J. Carter,[4] L. Donaldson,[4] H. Fujita,[2] Y. Fujita,[2] T. Hashimoto,[2] K. Hatanaka,[2] T. Ito,[2] A. Krugmann,[1] B. Liu,[2] Y. Maeda,[5] K. Miki,[2] R. Neveling,[6] N. Pietralla,[1] I. Poltoratska,[1] V. Yu. Ponomarev,[1] A. Richter,[1] T. Shima,[2] T. Yamamoto,[2] and M. Zweidinger[1]

[1]*Institut für Kernphysik, Technische Universität Darmstadt, D-64289 Darmstadt, Germany*
[2]*Research Center for Nuclear Physics, Osaka University, Ibaraki, Osaka 567-0047, Japan*
[3]*Department of Physics and Astronomy, Texas A&M University-Commerce, Commerce, Texas 75429, USA*
[4]*School of Physics, University of the Witwatersrand, Johannesburg 2050, South Africa*
[5]*Faculty of Engineering, Miyazaki University, Miyazaki 889-2192, Japan*
[6]*iThemba LABS, Somerset West 7129, South Africa*

(Received 6 November 2016; revised manuscript received 12 June 2017; published 2 November 2017)

The gamma strength function and level density of 1^- states in ^{96}Mo have been extracted from a high-resolution study of the $(\vec{p}, \vec{p}')$ reaction at 295 MeV and extreme forward angles. By comparison with compound nucleus γ decay experiments, this allows a test of the generalized Brink-Axel hypothesis in the energy region of the pygmy dipole resonance. The Brink-Axel hypothesis is commonly assumed in astrophysical reaction network calculations and states that the gamma strength function in nuclei is independent of the structure of the initial and final state. The present results validate the Brink-Axel hypothesis for ^{96}Mo and provide independent confirmation of the methods used to separate gamma strength function and level density in γ decay experiments.

DOI: 10.1103/PhysRevLett.119.182503

Introduction.—The gamma strength function (GSF) describes the average γ decay behavior of a nucleus. Its knowledge is required for applications of statistical nuclear theory in astrophysics [1], reactor design [2], and waste transmutation [3]. Although all electromagnetic multipoles contribute, the GSF is dominated by the $E1$ radiation with smaller contributions from $M1$ strength. Above particle threshold, it is governed by the isovector giant dipole resonance (IVGDR) but at lower excitation energies the situation is complex: In nuclei with neutron excess one observes the formation of the pygmy dipole resonance (PDR) [4] sitting on the low-energy tail of the IVGDR. The impact of low-energy $E1$ strength on astrophysical reaction rates and the resulting abundances in the r process have been discussed, e.g., in Refs. [5–7].

Most applications imply an environment of finite temperature, notably in stellar scenarios [8], and thus, reactions on initially excited states become relevant. Their contributions to the reaction rates are usually estimated applying the generalized Brink-Axel (BA) hypothesis [9,10], which states that the GSF is independent of the properties of the initial and final states and, thus, should be the same in γ emission and absorption experiments. Although historically formulated for the IVGDR, where it seems to hold approximately for not too high temperatures [11], nowadays, this is a commonly used assumption to calculate the low-energy $E1$ and $M1$ strength functions. Recent theoretical studies [12,13] put that into question demonstrating that the strength functions of collective modes built on excited states do show an energy dependence. However, numerical results for $E1$ strength functions obtained in Ref. [12] showed an approximate constancy as a function of excitation energy consistent with the BA hypothesis.

Recent work utilizing compound nucleus γ decay with the so-called Oslo method [14] has demonstrated independence of the GSF from excitation energies and spins of initial and final states in a given nucleus in accordance with the BA hypothesis once the level densities are sufficiently high to suppress large intensity fluctuations [15]. However, there are a number of experimental results which indicate violations of the BA hypothesis in the low-energy region. For example, the GSF in heavy deformed nuclei at excitation energies of 2–3 MeV is dominated by the orbital $M1$ scissors mode [16] and potentially large differences in $B(M1)$ strengths are observed between γ emission and absorption experiments [17–19]. At very low energies (<2 MeV), an increase of GSFs is observed in Oslo-type experiments [20,21] which, for even-even nuclei, cannot have a counterpart in ground state absorption experiments because of the pairing gap.

For the low-energy $E1$ strength in the region of the pygmy dipole resonance (PDR), the question is far from clear when comparing results from the Oslo method with photoabsorption data. Below particle thresholds, most information on the GSF stems from nuclear resonance fluorescence (NRF) experiments. A striking example of disagreement is the GSF of ^{96}Mo, where the results from the Oslo method [22,23] and from NRF [24] differ by factors 2–3 at excitation energies between 4 and 7 MeV. A problem with the NRF method is the experimentally unobserved

branching ratios to excited states. While many older analyses of NRF data assume that these are negligible, in Ref. [24], they are included by a Hauser-Feshbach calculation assuming statistical decay. The resulting corrections are sizable, reaching a factor of 5 close to the neutron threshold. On the other hand, there are indications of nonstatistical decay behavior of the PDR from recent measurements [25,26]. Violation of the BA hypothesis was also claimed in a simultaneous study of the (γ, γ') reaction and average ground state branching ratios [27] in ^{142}Nd (see, however, Ref. [28]). Clearly, information on the GSF—in particular in the energy region of the PDR—from an independent experiment is called for.

A new method for the measurement of complete $E1$ strength distributions—and, thereby, the $E1$ part of the GSFs—in nuclei from about 5 to 25 MeV has been developed using relativistic Coulomb excitation in polarized inelastic proton scattering at energies of a few hundred MeV and scattering angles close to 0° [29–33]. These data allow the dipole polarizability to be determined which provides important constraints on the neutron skin of nuclei and the poorly known parameters of the symmetry energy [34]. They also permit extraction of the $M1$ part of the GSF due to spin-flip excitations [35], which energetically overlap with the PDR strength. Furthermore, when performed with good energy resolution, the level density (LD) can be extracted in the excitation region of the IVGDR from the giant resonance fine structure independent of the GSF [36]. This allows an important test of the model-dependent decomposition of LD and GSF in the Oslo method [14].

Such a test has been performed for the case of ^{208}Pb [37], and good agreement of LDs deduced from the Oslo method and the (p, p') data was found. However, because of the extremely low LD of a doubly magic nucleus and the corresponding strong intensity fluctuations in a ground-state absorption experiment, the comparison of the GSFs in the PDR energy region remained inconclusive. Here, a study of an open-shell nucleus is reported, where the LD should be sufficiently high for a comparison with averaged quantities from the (p, p') experiment. The case of ^{96}Mo was selected for a critical examination of the above-discussed apparent violation of the BA hypothesis in the low-energy regime suggested by the NRF data [24].

Experiment.—The ^{96}Mo$(\vec{p}, \vec{p}')$ reaction was studied at RCNP, Osaka, Japan. Details of the experimental techniques can be found in Ref. [38]. A proton beam of 295 MeV with intensities of about 2 nA at 0° up to 6 nA at larger spectrometer angles and with an average polarization $P_0 \simeq 0.67$ impinged on a ^{96}Mo foil isotopically enriched to 96.7% with an areal density of 3 mg/cm^2. Data were taken with the Grand Raiden spectrometer [39] placed at 0° covering an angular acceptance of ±2.6° and excitation energies $E_x \simeq 5$–23 MeV. The energy resolution varied between 25 and 40 keV (FWHM). Normally (N) and longitudinally (L) polarized beams were used to measure the polarization transfer coefficients [40] $D_{NN'}$ and $D_{LL'}$, respectively. Additional data with unpolarized protons were taken for angles up to 6°.

Figure 1(a) displays the spectra taken at spectrometer angles 0°, 3°, and 4.5°. Besides discrete transitions at low excitation energies, a resonancelike structure around 8 MeV and the prominent IVGDR centered at $E_x \approx 16$ MeV are observed. The cross sections show a strong forward-angle peaking indicating the dominance of Coulomb excitation. The total spin transfer

$$\Sigma = \frac{3 - (2D_{NN'} + D_{LL'})}{4} \quad (1)$$

shown in Fig. 1(b) can be extracted from the measured polarization transfer observables. It takes a value of one for spin-flip ($\Delta S = 1$) and zero for nonspin-flip ($\Delta S = 0$) transitions at 0° [41], interpreted as $M1$ and $E1$ cross section parts, respectively. Values in between 0 and 1 result from the summation over finite energy bins (200 keV up to an excitation energy of 10 MeV and 500 keV above). The polarization transfer analysis (PTA) reveals the presence of a few spin-flip transitions between 5 and 7.5 MeV and a concentration of spin-flip strength in the energy region 7.5–10 MeV identified as the spin-$M1$ resonance in ^{96}Mo. Cross sections above 10 MeV are dominantly of $\Delta S = 0$ character, as expected for Coulomb excitation. These findings are consistent with the results in ^{208}Pb [29] and ^{120}Sn [32].

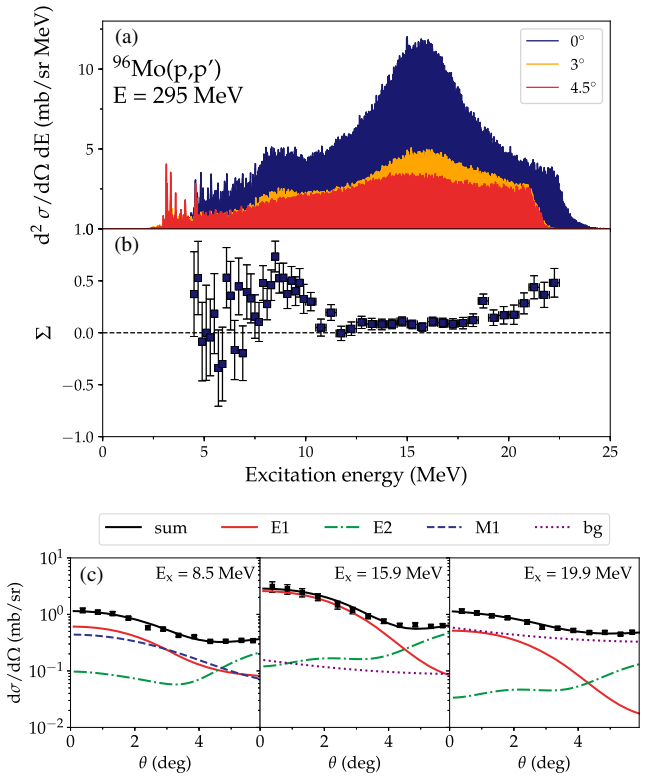

FIG. 1. (a) Spectra of the ^{96}Mo$(\vec{p}, \vec{p}')$ reaction at $E_p = 295$ MeV with the spectrometer placed at 0° (blue), 3° (yellow), and 4.5° (red). (b) Total spin transfer Σ, Eq. (1). (c) Examples of the MDA for selected energy bins.

The $\Delta S = 1$ strength observed at high E_x can be understood to arise from quasifree scattering [42].

Alternatively, a multipole decomposition analysis (MDA) was performed for angular distributions of the cross sections in the PDR and GDR regions. For this purpose, angular cuts were applied to the spectra of Fig. 1(a) providing four data points each. The MDA followed the approach described in Refs. [29,30] closely. For the nuclear background, the empirical parametrization found for ^{208}Pb [43] was adopted assuming the same momentum transfer dependence. Figure 1(c) presents representative examples of the MDA for 200 keV excitation energy bins at different excitation energies. They demonstrate that, in the low-energy bump, $M1$ contributions are sizable while $E1$ dominates in the energy region of the IVGDR. At even higher energies, the nuclear background becomes dominant.

The relative yield R of spin-flip and nonspin-flip cross sections resulting from the MDA and PTA for $E_x \leq 11$ MeV is compared in Fig. 2. The two completely independent decomposition methods lead to consistent results within error bars except for one energy bin around 8.5 MeV. In the following, $E1$ and $M1$ cross sections averaged over both decomposition methods are considered for excitation energies up to 11 MeV. At higher E_x, only the MDA results are taken since the $\Delta S = 0$ part of the nuclear background, which cannot be distinguished in the PTA, becomes relevant.

Gamma strength function.—The GSF for electric or magnetic transitions $X \in \{E, M\}$ with multipolarity λ is related to the photoabsorption cross section $\langle \sigma_{\mathrm{abs}}^{X\lambda} \rangle$ by

$$f^{X\lambda}(E, J) = \frac{2J_0 + 1}{(\pi\hbar c)^2 (2J + 1)} \frac{\langle \sigma_{\mathrm{abs}}^{X\lambda} \rangle}{E_\gamma^{2\lambda-1}}, \qquad (2)$$

where E_γ denotes the γ energy and J, J_0 are the spins of excited and ground state, respectively [44]. For absorption experiments $E_x = E_\gamma$. The brackets $\langle\rangle$ indicate averaging over an energy interval. In practice, only $E1$ and $M1$ transitions provide sizable contributions to the total GSF. The Coulomb excitation cross sections representing the $E1$ part of the GSF were converted to equivalent photoabsorption cross sections using the virtual photon method [45]. The virtual photon spectrum exhibits a strong energy dependence, which amounts to a factor of 10 for the energy region 6–20 MeV covered in the present experiment. It was calculated in an eikonal approach [46] and integrated over the solid angle covered by the experiment. The $M1$ cross sections from Fig. 2 were converted to reduced transition strengths and the corresponding $M1$ photoabsorption cross sections with the approach described in Refs. [35,47].

The sum approximating the total GSF in ^{96}Mo is displayed in Fig. 3(a) as red circles for $E_\gamma = 6$–20 MeV. The error bars include statistical (dominating the PTA) and systematic (dominating the MDA) uncertainties The result is compared with (^{3}He, ^{3}He$'\gamma$) [22,23] (open circles), (γ, xn) [48] (grey squares), (γ, n) [49] (blue upward triangles), and (γ, γ') data corrected for unobserved branching ratios [24] (black circles). Above threshold, there is overall fair agreement with the data from Refs. [48,49] except that the present experiment finds somewhat larger photoabsorption cross sections around the maximum of the IVGDR.

Below S_n, the GSF from the present work lies in between the Oslo and the (γ, γ') experiment. An expanded view of

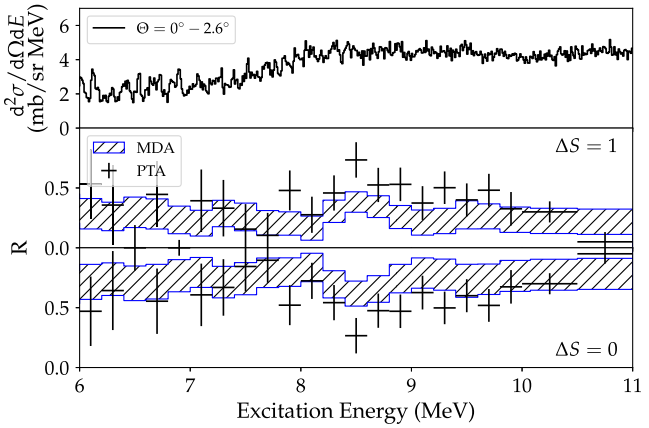

FIG. 2. Relative yield R of nonspin-flip ($\Delta S = 0$) and spin-flip ($\Delta S = 1$) cross section parts of the ^{96}Mo($\vec{p}, \vec{p}'$) spectrum in the excitation energy region 6–11 MeV based on the MDA and PTA, respectively. Agreement between the two independent methods is observed within error bars.

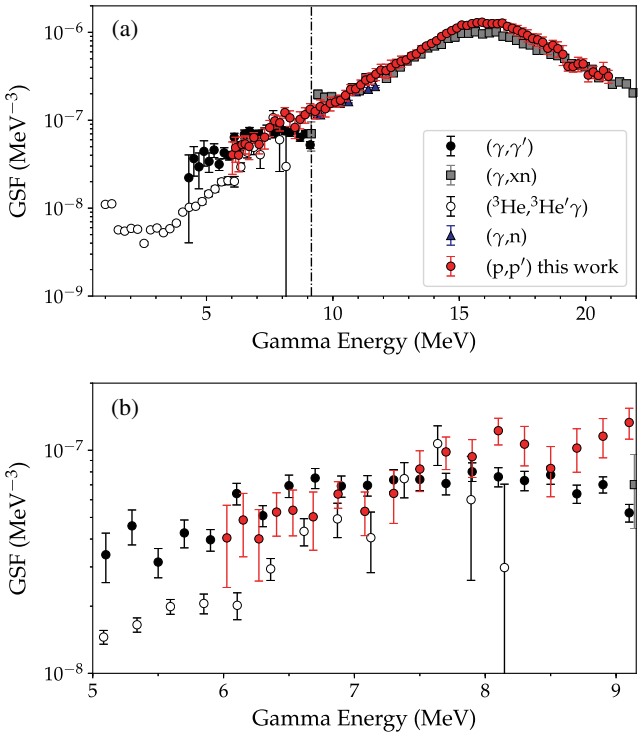

FIG. 3. (a) GSF of ^{96}Mo from the present work (red circles) compared with (^{3}He, ^{3}He$'\gamma$) [22,23] (open circles), (γ, xn) [48] (grey squares), (γ, n) [49], (blue upward triangles), and (γ, γ') [24] data including a statistical model correction for unobserved branching ratios (black circles) (b) Expanded range from 5 MeV to neutron threshold.

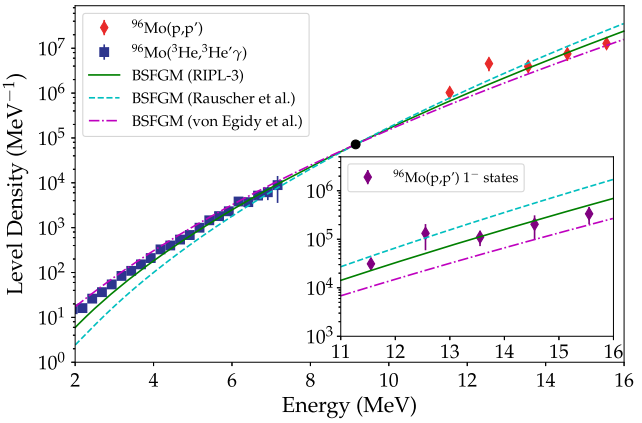

FIG. 4. Total LD in ^{96}Mo deduced from the fine structure of the (p, p') data in the energy region of the IVGDR (red diamonds) compared with the results from the (^{3}He, ^{3}He′γ) Oslo experiment (blue squares) [22,23]. The black circle point stems from s-wave resonance neutron capture [49]. BSFG models normalized to the value at S_n are shown as green solid [44], cyan dashed [53], and purple dashed-dotted [54] lines. The inlet shows the LD of 1^- states in comparison with absolute predictions of the models.

the GSF results between 5 MeV and the neutron threshold $S_n = 9.154$ MeV is displayed in Fig. 3(b). The (p, p') and (^{3}He, ^{3}He′γ) results agree within error bars except for the two lowest excitation energies analyzed in the present data. However, these two data points suffer from limited statistics. The (γ, γ') results [24] agree in the 7–8 MeV excitation energy region 7–8 MeV but, clearly, underestimate the present results at higher E_x. At lower E_x, they are systematically at the upper limit of the present results (and sometimes exceed it) and are significantly larger than the Oslo results. The deviations from the present results may arise from the modeling of the large atomic background in the spectra and/or the specific choice of level densities for the simulation of the γ decay cascades [50].

Level density.—Since only the product of GSF and LD is measured by the Oslo method [14], it relies on external data for their decomposition. Thus, an independent check of the LD results for ^{96}Mo is of high importance. The good energy resolution of the present data permits an extraction of the LD of $J^\pi = 1^-$ states applying a fluctuation analysis to the fine structure of the IVGDR. Details of the method can be found in Refs. [36,51,52]. We note that the method is based on the assumption of a single class of excited states in the spectrum. This presently limits the application to the energy region of the IVGDR while, at lower excitation energies, 1^- and 1^+ states coexist, since the PDR and the spin $M1$ strength overlap. The LD of $J^\pi = 1^-$ states between 11 and 16 MeV is displayed in the inset of Fig. 4 in comparison with three widely used systematic parametrizations [44,53,54] of the phenomenological backshifted Fermi gas (BSFG) model (see Table I). The BSFG parameters deduced from the RIPL-3 data base [44] provide a good description, while absolute values from the other models are too high [53] or too low [54].

TABLE I. Level density (a), backshift (Δ) and spin cutoff (σ) parameters of the BSFG model predictions for ^{96}Mo shown in Fig. 4.

References	a (MeV^{-1})	Δ (MeV)	σ(11.5 MeV) ($\hbar$)	σ(15.5 MeV) ($\hbar$)
[44]	11.25	1.14	5.32	5.77
[53]	12.45	1.48	5.01	5.45
[54]	9.56	0.82	4.20	4.42

In order to compare with the Oslo results, the 1^- LD is converted to a total LD using a spin distribution function

$$f(J) \simeq \frac{2J+1}{2\sigma^2} \exp\left(-\frac{(J+\frac{1}{2})^2}{2\sigma^2}\right), \quad (3)$$

where σ denotes the spin cutoff parameter. Note that slightly different definitions of $f(J)$ are used in Refs. [44,53,54]. A parity dependence is neglected in accordance with the results of Ref. [55]. Values of σ for the experimental energy range using the respective definitions are given in Table I. The model dependence of the conversion to total LD is taken into account by averaging over the results from the three BSFG parameter sets and taking their variance as a measure of the model uncertainty. The resulting LD (red diamonds) is presented in Fig. 4 together with the Oslo results at lower excitation energies (blue squares) and s-wave neutron capture (black circle) [49]. The BSFG models are normalized to the value at S_n. In particular, the RIPL-3 parameters [44] provide a good description of all data over a large excitation energy range, consistent with a similar analysis for ^{208}Pb [37].

Conclusions.—A new approach to test the Brink-Axel hypothesis is presented based on a study of the $(\vec{p}, \vec{p}')$ reaction at 295 MeV and extreme forward angles. The extracted gamma strength function for the test case, ^{96}Mo, agrees with results of compound nucleus γ decay experiments [22,23] indicating that the BA hypothesis holds in the energy region of the PDR, in contrast to results from the (γ, γ') reaction [24] and the claims of Ref. [27]. This is an important finding since the BA hypothesis constitutes a general presupposition for astrophysical reaction network calculations. The high energy resolution and selectivity of the data permits an extraction of the LD at excitation energies above the neutron threshold hardly accessible by other means. A consistent description of the LD with those of the γ decay experiments can be achieved within BSFG models providing independent confirmation of the methods used to separate GSF and LD in Oslo-type experiments.

While the present results support a use of the BA hypothesis for statistical model calculations of reaction cross sections in finite temperature environments, a general statement requires a systematic comparison of GSFs derived from γ absorption and emission experiments in the energy range of the PDR over a broad range of nuclei. For example, the role of deformation needs to be explored by comparing spherical and well-deformed cases with the

present results for the moderately deformed ^{96}Mo. Work along these lines is under way.

We are indebted to the RCNP for providing excellent beams. Discussions with E. Grosse, M. Guttormsen, A. C. Larsen, R. Schwengner, and S. Siem are gratefully acknowledged. This work has been supported by the Deutsche Forschungsgemeinschaft under Contract No. Sonderforschungsbereich 1245 and by the Japan Ministry of Education, Culture, Sports, Science and Technology Grants in Aid for Scientific Research Grant No. JP25105509. C. A. B. acknowledges support by the U.S. Department of Energy Grant No. DE-FG02-08ER41533 and the U.S. National Science Foundation (NSF) Grant No. 1415656.

*vnc@ikp.tu-darmstadt.de

[1] M. Arnould, S. Goriely, and K. Takahashi, Phys. Rep. **450**, 97 (2007).
[2] M. B. Chadwick *et al.*, Nucl. Data Sheets **112**, 2887 (2011).
[3] M. Salvatore and G. Palmiotti, Prog. Part. Nucl. Phys. **66**, 144 (2011).
[4] D. Savran, T. Aumann, and A. Zilges, Prog. Part. Nucl. Phys. **70**, 210 (2013).
[5] S. Goriely, E. Khan, and M. Samyn, Nucl. Phys. **A739**, 331 (2004).
[6] E. Litvinova, H. P. Loens, K. Langanke, G. Martínez-Pinedo, T. Rauscher, P. Ring, F.-K. Thielemann, and V. Tselyaev, Nucl. Phys. **A823**, 26 (2009).
[7] I. Daoutidis and S. Goriely, Phys. Rev. C **86**, 034328 (2012).
[8] M. Wiescher, F. Käppeler, and K. Langanke, Annu. Rev. Astron. Astrophys. **50**, 165 (2012).
[9] D. M. Brink, Ph.D. thesis, Oxford University, 1955.
[10] P. Axel, Phys. Rev. **126**, 671 (1962).
[11] P. F. Bortignon, A. Bracco, and R. A. Broglia, *Giant Resonances: Nuclear Structure at Finite Temperature* (Harwood Academic, Amsterdam, 1998).
[12] C. W. Johnson, Phys. Lett. B **750**, 72 (2015).
[13] N. Quang Hung, N. Dinh Dang, and L. T. Quynh Huong, Phys. Rev. Lett. **118**, 022502 (2017).
[14] A. Schiller, L. Bergholt, M. Guttormsen, E. Melby, J. Rekstad, and S. Siem, Nucl. Instrum. Methods Phys. Res., Sect. A **447**, 498 (2000).
[15] M. Guttormsen, A. C. Larsen, A. Görgen, T. Renstrom, S. Siem, T. G. Tornyi, and G. M. Tveten, Phys. Rev. Lett. **116**, 012502 (2016).
[16] D. Bohle, A. Richter, W. Steffen, A. E. L. Dieperink, N. Lo Iudice, F. Palumbo, and O. Scholten, Phys. Lett. B **137**, 27 (1984).
[17] K. Heyde, P. von Neumann-Cosel, and A. Richter, Rev. Mod. Phys. **82**, 2365 (2010).
[18] M. Guttormsen *et al.*, Phys. Rev. Lett. **109**, 162503 (2012).
[19] C. T. Angell, R. Hajima, T. Shizuma, B. Ludewigt, and B. J. Quiter, Phys. Rev. Lett. **117**, 142501 (2016).
[20] A. Voinov, E. Algin, U. Agvaanluvsan, T. Belgya, R. Chankova, M. Guttormsen, G. E. Mitchell, J. Rekstad, A. Schiller, and S. Siem, Phys. Rev. Lett. **93**, 142504 (2004).
[21] A. C. Larsen *et al.*, Eur. Phys. J. Web Conf. **66**, 07014 (2014).
[22] M. Guttormsen *et al.*, Phys. Rev. C **71**, 044307 (2005).
[23] A. C. Larsen and S. Goriely, Phys. Rev. C **82**, 014318 (2010).
[24] G. Rusev *et al.*, Phys. Rev. C **79**, 061302 (2009).
[25] C. Romig *et al.*, Phys. Lett. B **744**, 369 (2015).
[26] B. Löher *et al.*, Phys. Lett. B **756**, 72 (2016).
[27] C. T. Angell, S. L. Hammond, H. J. Karwowski, J. H. Kelley, M. Krtička, E. Kwan, A. Makinaga, and G. Rusev, Phys. Rev. C **86**, 051302(R) (2012).
[28] C. T. Angell, S. L. Hammond, H. J. Karwowski, J. H. Kelley, M. Krtička, E. Kwan, A. Makinaga, and G. Rusev, Phys. Rev. C **91**, 039901(E) (2015).
[29] A. Tamii *et al.*, Phys. Rev. Lett. **107**, 062502 (2011).
[30] I. Poltoratska *et al.*, Phys. Rev. C **85**, 041304(R) (2012).
[31] A. M. Krumbholz *et al.*, Phys. Lett. B **744**, 7 (2015).
[32] T. Hashimoto *et al.*, Phys. Rev. C **92**, 031305(R) (2015).
[33] J. Birkhan *et al.*, Phys. Rev. Lett. **118**, 252501 (2017).
[34] Bao-An Li, A. Ramos, G. Verde, and I. Vidaña, Eur. Phys. J. A **50**, 9 (2014).
[35] J. Birkhan, H. Matsubara, P. von Neumann-Cosel, N. Pietralla, V. Yu. Ponomarev, A. Richter, A. Tamii, and J. Wambach, Phys. Rev. C **93**, 041302(R) (2016).
[36] I. Poltoratska, R. W. Fearick, A. M. Krumbholz, E. Litvinova, H. Matsubara, P. von Neumann-Cosel, V. Yu. Ponomarev, A. Richter, and A. Tamii, Phys. Rev. C **89**, 054322 (2014).
[37] S. Bassauer, P. von Neumann-Cosel, and A. Tamii, Phys. Rev. C **94**, 054313 (2016).
[38] A. Tamii *et al.*, Nucl. Instrum. Methods Phys. Res., Sect. A **605**, 326 (2009).
[39] M. Fujiwara *et al.*, Nucl. Instrum. Methods Phys. Res., Sect. A **422**, 484 (1999).
[40] G. G. Ohlsen, Rep. Prog. Phys. **35**, 717 (1979).
[41] T. Suzuki, Prog. Theor. Phys. **103**, 859 (2000).
[42] F. T. Baker *et al.*, Phys. Rep. **289**, 235 (1997).
[43] I. Poltoratska, Ph.D. thesis D17, TU Darmstadt, 2011, http://tuprints.ulb.tu-darmstadt.de/2671.
[44] R. Capote *et al.*, Nucl. Data Sheets **110**, 3107 (2009).
[45] C. A. Bertulani and G. Baur, Phys. Rep. **163**, 299 (1988).
[46] C. A. Bertulani and A. M. Nathan, Nucl. Phys. **A554**, 158 (1993).
[47] M. Mathy, J. Birkhan, H. Matsubara, P. von Neumann-Cosel, N. Pietralla, V. Yu. Ponomarev, A. Richter, and A. Tamii, Phys. Rev. C **95**, 054316 (2017).
[48] H. Beil, R. Bergère, P. Carlos, A. Leprêtre, A. De Miniac, and A. Veyssiere, Nucl. Phys. **A227**, 427 (1974).
[49] H. Utsunomiya *et al.*, Phys. Rev. C **88**, 015805 (2013).
[50] G. Rusev *et al.*, Phys. Rev. C **77**, 064321 (2008).
[51] Y. Kalmykov *et al.*, Phys. Rev. Lett. **96**, 012502 (2006).
[52] I. Usman *et al.*, Phys. Rev. C **84**, 054322 (2011).
[53] T. Rauscher, F.-K. Thielemann, and K.-L. Kratz, Phys. Rev. C **56**, 1613 (1997).
[54] T. von Egidy and D. Bucurescu, Phys. Rev. C **80**, 054310 (2009).
[55] Y. Kalmykov, C. Özen, K. Langanke, G. Martínez-Pinedo, P. von Neumann-Cosel, and A. Richter, Phys. Rev. Lett. **99**, 202502 (2007).